Non-local effects of large eddies in surface layer*

ESAU I.N.
Nansen Environmental and Remote Sensing Center,
Edvard's Griegvei 3A, 5059 Bergen, Norway
igore@nersc.no

27 декабря 2003 г.

The turbulent mixing in modern large scale models is parameterized through turbulent exchange coefficients. These coefficients are calculated following the classical logarithmic law in high Reynolds number boundary layers, where effect of large eddies are neglected. This study demonstrates that these effects are significant. Large eddies are essentially non-local, therefore, not only surface boundary conditions but also conditions at the PBL top must be included in the expression for exchange coefficients. Conditions at the PBL top appear through an imposed stability parameter, μ_N, which characterizes the effect of stability of the free atmosphere. Restrictions on the eddy size significantly reduce turbulent mixing comparative to predictions of the classical theories. The study results in development of a new non-local parameterization for large-scale modeling.

1. Introduction

Despite of complexity of the earth's surface, widely used parameterizations of the turbulent exchange remain rather simple [1]. The most of the large scale models (LSMs) participating in the atmospheric model intercomparison program (AMIP) rely on surface turbulent exchange coefficients (STECs) representing the influence of boundary conditions on the turbulent atmospheric flow. This approach has been developed from studies of von Karman and Prandtl. They derived the famous logarithmic law of the wall (log-law) for neutrally stratified boundary layer flow at high Reynolds number

$$\frac{d|\mathbf{u}|}{dz} = \frac{u_*}{\kappa z}, \tag{1}$$

where u_* is the turbulent stress velocity, κ is the von Karman constant and z is the height above the surface. A number of atmospheric studies [2] seems to support the log-law.

In the context of the turbulence exchange problem, the log-law is the cornerstone of the parameterization of the STECs

$$C_D = \frac{\tau_s}{\mathbf{u}^2}, \qquad C_H = \frac{F_{bs}}{|\mathbf{u}|\Delta\Theta}, \qquad C_M = \frac{F_{qs}}{|\mathbf{u}|\Delta q}, \tag{2}$$

where $\tau_s = u_*^2$, F_{bs} and F_{qs} are the turbulent momentum, heat and scalar fluxes at the surface, $\mathbf{u}$ is the flow velocity and $\Delta\Theta$, Δq are bulk gradients of potential temperature and scalar. This study considers only C_D, the parameterization of the STEC for momentum in the

*The study was supported by Norwegian ROLARC and MACESIS projects.

conventionally neutral PBL. The STEC in convective and stable PBLs may be calculated using correction functions [3]. These functions follow from the Monin-Obukhov similarity [4]. They will not be touched here. The Monin-Obukhov similarity [5] is not so well grounded as the log-law itself. Actually, data demonstrates too large scatter especially in the stably stratified PBL.

Eq. (2) can be rewritten as

$$C_D = \frac{\kappa^2}{\ln(1 + z/z_0)}, \tag{3}$$

where z_0 is surface roughness. Here, the only dimensionless parameter is z/z_0. As the matter of fact, there were many attempts to introduce additional dimensionless parameters into the atmospheric log-law. Blackadar [6] proposed z/H as the additional dimensionless parameter, where H is the PBL depth. Make use of the Rossby-Montgomery [7] relation for H provides dependence of the exchange coefficients on the surface Rossby number. This dependence is known from data analysis [8]. Byun [9] recognized the role of the ambient atmospheric stratification. Zilitinkevich and Calanca [10] introduced into the log-law a new imposed stability parameter, $\mu_N = N/|f|$, where f is the Coriolis parameter and N is the Brunt-Väsälä frequency. N characterizes the ambient stratification of the atmosphere above the PBL. Zilitinkevich and Esau [11] showed that application of μ_N considerably reduces the scatter of H in the conventionally neutral PBL. Zilitinkevich *et al.* [4] developed an advanced parameterization of the STECs in stable atmospheric conditions, which accounts for μ_N in the frameworks of the Monin-Obukhov similarity approach. The parameterization is still to be tested in real LSMs.

There is also another approach to possible modifications of the log-law. It consider the von Karman constant κ as a variable parameter. Atmospheric and laboratory measurements [2] provide rather uncertain values of κ. Moreover, recent publications [12], [13] revealed regular dependence of κ on the roughness Reynolds number.

The natural question is what kind of motions achieve direct interactions between the stratified free atmosphere and the near-neutral surface layer. In the turbulent PBL, the only possible candidates are large three-dimensional eddies, i.e. the eddies with the size of the PBL depth. Following Zilitinkevich [14], such large eddies are denoted as non-local turbulence since the local state of the turbulent flow does not determine their properties.

The large eddies have been neglected for long time. Bradshaw [15] considered the large eddies as an inactive part of turbulent motions, which do not exert the turbulent stress and do not mix heat and moisture. Robinson [16] considered only small scale near-wall eddies in his review of coherent structures in low and moderate Re boundary layers. This view was mechanically accepted in consideration of coherent structures in the high Re PBL. Recently, Hunt and Morrison [17] have argued this view. They pointed out that the nature of high Re turbulence is different from the nature of low and moderate Re turbulence. Although small scale turbulence is intense in the PBL, the large eddies are also important. The large eddies seem to be even more important than it has been usually thought [18]. Hunt and Carlotti [19] published several distinct analytical predictions for the behavior of turbulence statistics in the high Re PBL. To a great surprise, atmospheric measurements appear to be in good agreement with the predictions [20].

This study deals only with the large eddies in the turbulence resolving simulations (LES) of the conventionally neutral PBL. It gives a possibility to present in one publication structure and statistical properties of the large eddies as well as their direct effect on C_D. This study questions some basic physical assumptions of the classical turbulence theory. These

assumptions are presented in Section 2. Section 3. discusses effects of the large eddies in the PBL. Section 4. discusses one way to account for the non-local turbulence in an improved STEC parameterization. Section 5. outlines conclusions of this study.

2. Basic assumptions in turbulence exchange parameterization

Several strong physical assumptions stand behind simple Equations (1) and (2). In viscous fluid, strains of individual fluid elements give rise to stresses analogues to those in elastic media. One can adapt the formalism of the elastic theory where the fluid velocity, $\mathbf{u}$, is used instead of displacements [21]. We cannot use the velocity itself since it is not an invariant with respect to coordinate transforms. Therefore, one can right for the turbulent stress

$$\tau = K_m \frac{\partial \mathbf{u}}{\partial z}, \tag{4}$$

where K_m is a proportionality coefficient known as the eddy viscosity. It is reasonable to assume that turbulent mixing in the surface layer is due to small scale eddies. The Richardson's assumption is that the small eddies act on the large eddies in the same way as the molecular motions act on the small eddies themselves. The Richardson's assumption verifies the application of the Fourier law for molecular diffusivity

$$K_m = C_D \Delta z |\mathbf{u}(z) - \mathbf{u}(0)|, \tag{5}$$

where C_D is an exchange coefficient. Substitution of Eq. (5) into Eq. (4) and accounting for the non-slip boundary conditions, $\mathbf{u}(0) = 0$, immediately result in Eq. (2). The latter contains the unknown variable $\mathbf{u}(z)$. Make use of the log-law in Eq. (1), one can eliminate the velocity

$$C_D = \frac{|\tau|}{\mathbf{u}^2(z)} = \frac{u_*^2}{\mathbf{u}^2(z)} = \frac{\kappa \mathbf{u}^2(z)}{\mathbf{u}^(z) \ln(1 + z/z_0)} = \frac{\kappa}{\ln(1 + z/z_0)}. \tag{6}$$

This is Eq. (3), which parameterizes the STEC in the LSM. Here, C_D depends only on one dimensionless parameter z/z_0. Figure 1 shows the dependence $C_D^{LES} = u_*^2/\mathbf{u}^2(z)$ on z/z_0 in the surface layer. Data is from a database [22] of conventionally neutral LES runs. The large data scatter suggests that z/z_0 is not the only dimensionless parameter in the neutral PBL.

To identify the problem, let us reconsider Eq. (4) again. One can rewrite Eq. (4) as

$$\frac{\partial \mathbf{u}(z)}{\partial z} = \frac{\tau}{K_m}. \tag{7}$$

Dimensional analysis suggests that $K_m = l \cdot u_s$ is a combination of length and velocity scales. Von Karman proposed $l = \kappa z$ and $u_s = u_*$ on basis of his laboratory experiments. It will immediately give the log-law in Eq. (1) and, therefore, Eq. (3). The von Karman assumptions are strongly based on the fact that eddies are generated at the wall. Such eddies cannot be larger than the distance to the wall. The small eddies have short life time. The work of pressure quickly forces the eddy evolution to the isotropic and homogeneous state.

3. External scaling in the PBL

Turbulence in the PBL is rather different from von Karman's and Kolmogorov's turbulence. Indeed, there is always enough room for energetic large eddies. The wind shear is responsible

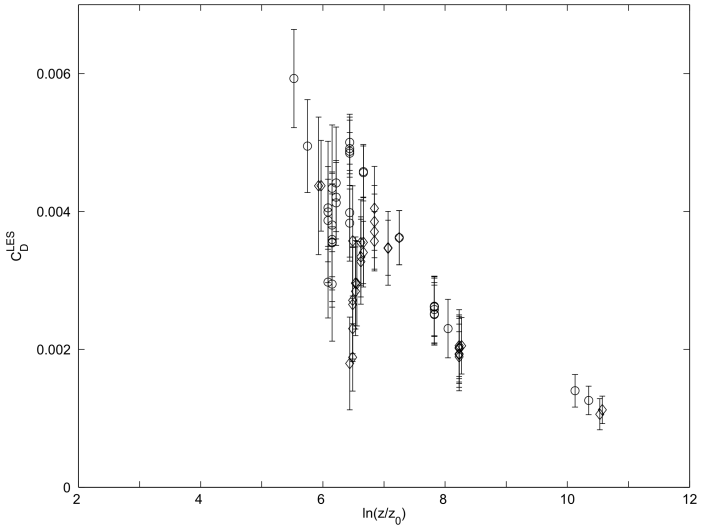

Рис. 1. The dependence of the surface turbulent exchange coefficient C_D^{LES} on the dimensionless parameter z/z_0. C_D^{LES} is calculated from the LES database of the conventionally neutral PBL runs: $\circ$ at $z = 40$ m.; $\diamond$ at $z = 60$ m. The lines denotes 96% internal of the statistical confidence (three standard deviation of the data scatter).

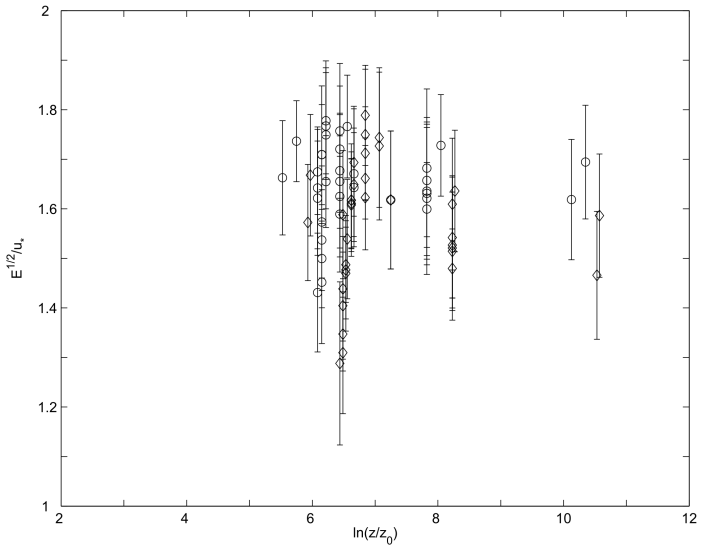

Рис. 2. The dependence of the normalized mean amplitude of the velocity fluctuations $E^{1/2}/u_*$ on the dimensionless parameter z/z_0. $E^{1/2}/u_*$ is calculated from the LES database of the conventionally neutral PBL runs. Symbols and lines are the same as in Fig. 1.

for significant anisotropy of large eddies. Due to this anisotropy, the horizontal components of velocity, u and v, still retain the Kolmogorov's similarity on large and even very large scales [23]. However, the surface blocks the vertical component of velocity, w. This blocking effect should be important for large eddies with scales $\Lambda > z$. The small eddies would be insensitive to the blocking. Figure 3 provides a look on scale composition of the turbulent stress, $\tau = \int S_{uw}(k)dk$, and the longitudinal and vertical components of velocity fluctuations, $(u')^2 = \int S_{uu}(k)dk$ and $(w')^2 = \int S_{ww}(k)dk$, in the surface layer. It shows spatial spectra in the direction normal to the direction of $\mathbf{u}_g$. Despite of the expected dominance of the small scales, Fig. 3 reveals dominance of large scales in the composition of the turbulent stress. The PBL depth decreases more than 10 times from the case with $\mu_N = 1$ to the case with $\mu_N = 350$. The maximum of S_{ww} shifts significantly towards smaller scales from $\sim 2 \quad kz$ in the panel (a) to $\sim 6 \quad kz$ in the panel (c). However, the scales of the turbulent stress does not follow this tremendous decrease of isotropic turbulence scales. The turbulent stress has the maximum at about $0.9 \quad kz$ in the case with $\mu_N = 1$ and at about $2.5 \quad kz$ in the case with $\mu_N = 350$. It suggests that the turbulent stress is mainly sensitive to the scale of the largest eddies in the PBL. The largest eddies vary their degree of anisotropy in respond to limiting the PBL vertical scale.

This spectral analysis allows for a tentative conclusion that the large eddies play an important role in the surface turbulence stress composition. This analysis also suggests that the vertical scale of the large eddies is comparable with the PBL depth. Therefore, it is reasonable to consider the PBL depth, H, as an external mixing length scale. Figure 4 shows the surface turbulent stress, τ_s, as a function of the PBL depth. It is clearly seen that τ_s is rapidly decreases with decrease of the PBL depth. The instant structure of $\tau_s/max(\tau_s)$ at 60 m. is shown in Figure 5 for three cases $\mu_N = 1$ (a), $\mu_N = 100$ (b) and $\mu_N = 350$ (c). It is possible to see that τ_s is more concentrated in the shallow PBL in Fig. 5 (b) and (c). Here, only relatively small spots and strips of the flow participate in the instant exchange of momentum. Contrary, Fig 5 (a) shows that the large part of the flow participates in the instant exchange of momentum in the deep PBL. The most active turbulent exchange is related to edges of large eddies, where fluid moves in an almost vertical direction. The large eddies in the shallow PBL are strongly anisotropic. Therefore, they have sharper edges with strong turbulent exchange. The large eddies in the deep PBL are isotropic. They do not have sharp edges. Therefore, the turbulent exchange is more equally distributed over the surface. Figure 6 gives a sketch of the turbulent stress due to large eddies in both shallow and deep PBLs.

Three parameters determine the PBL depth in the earth's atmosphere. Two of them are well known. They are the Coriolis parameter, f, and the geostrophic wind speed, $|\mathbf{u}_g|$. The third parameter appears in Zilitinkevich's theory of non-local turbulence [14]. It is imposed stability of the atmosphere immediately above the PBL. The strength of the stratification can be measured by the potential temperature gradient, $\nabla_z\Theta$, or the Brunt-Väisälä frequency, N. Thus, one can introduce an external dimensionless parameter – the imposed stability parameter – as the combination $\mu_N = N/|f|$. The imposed stability parameter appears in the generalized expression for the PBL depth [11]

$$H = C_H \frac{u_*}{|f|}, \quad \text{where} \quad C_H = C_R(1 + C_0\mu_N)^{-1/2}. \tag{8}$$

Here, $C_R = 0.67 \pm 0.08$ and $C_0 = 25 \pm 10$ are empirical constant obtained from the LES database. The imposed stability is actually the controlling factor of the PBL depth in the

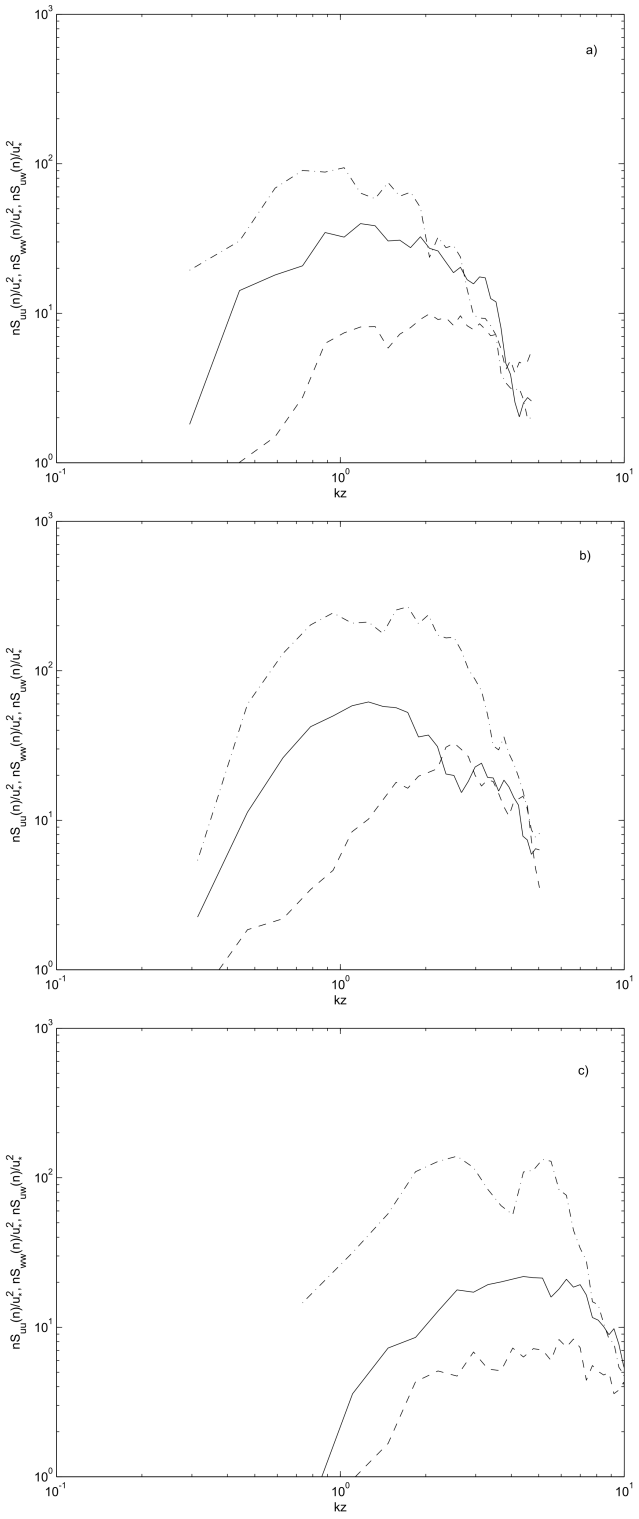

Рис. 3. Transverse spatial spectra of normalized longitudial, S_{uu} (solid line), and vertical, S_{ww} (dashed line), fluctuations of velocity as well as normalized turbulent stress, S_{uw} (dot-dashed line). The spectra are plotted versus normalized spatial wavenumber, $kz = 2\pi zn/L_y$, where $z \approx 60$ m. is the height above surface, n is the number of wavelengths in the computational domain of the size L_y. The panel (a) shows the spectra in the LES run with $\mu_N = 1$; the panel (b) – $\mu_N = 100$; the panel (c) – $\mu_N = 350$.

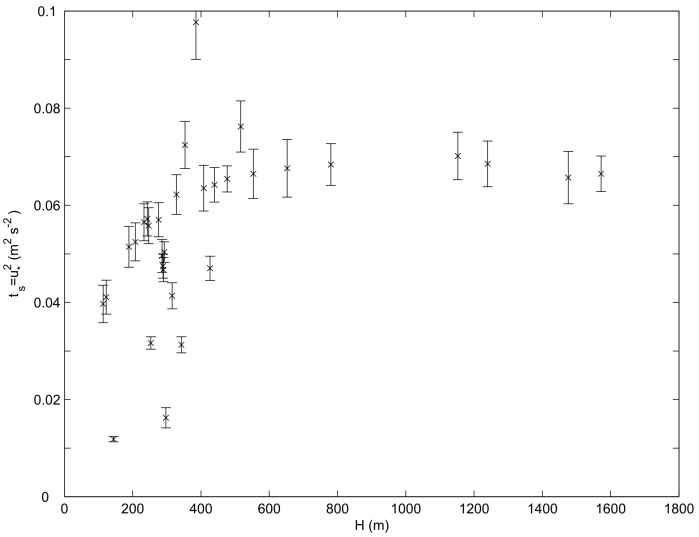

Рис. 4. The dependence of the turbulent surface stress, $\tau_s = u_*^2$ on the PBL depth H. The lines denotes 96% internal of the statistical confidence (three standard deviation of the data scatter).

atmospheric range of $N \sim 10^{-2}$ s^{-1}.

Deep boundary layers in Fig. 4 do not show the surface stress dependence on the PBL depth. The margin lays at about $\Lambda \approx 600$ m. scale. It indicates the largest vertical scale of coherent eddies in the neutral PBL. A principal orthogonal decomposion (POD) analysis [25] retrieves the typical shape and scale of the most energetic coherent eddies in the flow. Such eddies exert the main part of the turbulent stress. Figure 7 visualizes the statistically mean coherent eddy using a vorticity isosurface and streamlines of the eddy-induced secondary flow. It is obvious that the independent POD analysis provides the coherent eddy of the same $\Lambda \approx 600$ m. scale. Thus, the PBL depth limits the surface turbulent stress only until $H < \Lambda$. In deeper PBLs, which are rarely exist in nature, the limiting factor is the scale of the coherent structures. The latter depends largely on the surface roughness [24] and the Coriolis parameter [25].

4. Non-local turbulence exchange parameterization

It is possible to calculate the STEC from the LES database using Eq. (2) directly. Figure 8 shows variations of C_D with respect to the PBL depth. These variations demonstrate the same tendencies as the values of τ_s. The values of C_D are highly variable in the shallow PBLs and nearly constant in the deep PBLs. The margin of these two types of behavior is found again at about $\Lambda \approx 600$ m. Similarity in the behavior of C_D and $E^{1/2}/u_*$ versus H gives a strong support to the idea that H is another length scale relevant to the STEC.

Blackadar [6] incorporated the PBL depth into the log-law interpolating reciprocals

$$\frac{1}{l} = \frac{1}{z + z_0} + \frac{C_E}{H}, \tag{9}$$

where C_E is a dimensionless constant, which accounts for the relative significance of large eddies in the PBL. In this work, C_E is considered as an empirical constant. Physically, it

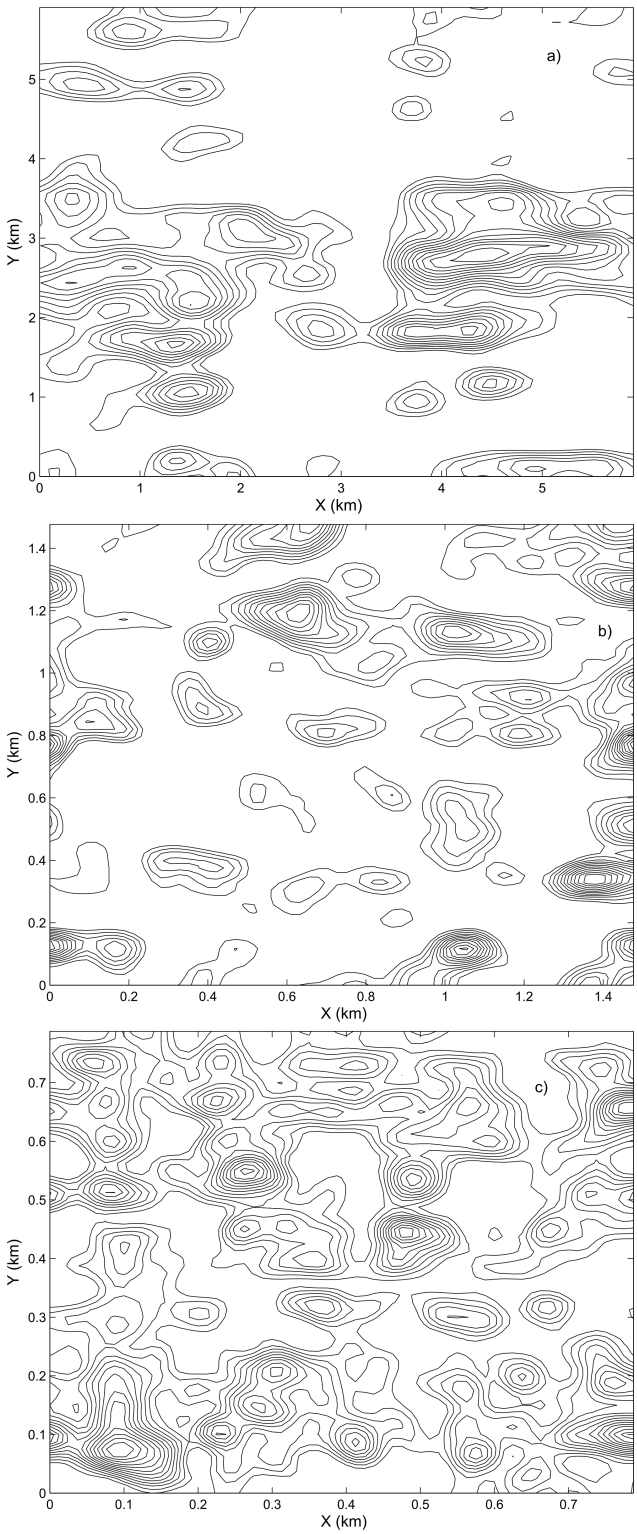

Рис. 5. The normalized resolved turbulent stress $\tau_s / \max(\tau_s)$ at $z \approx 60$ m. Contours start from 0.35 with the increment 0.05. Cases (a),(b) and (c) as in Fig. 3.

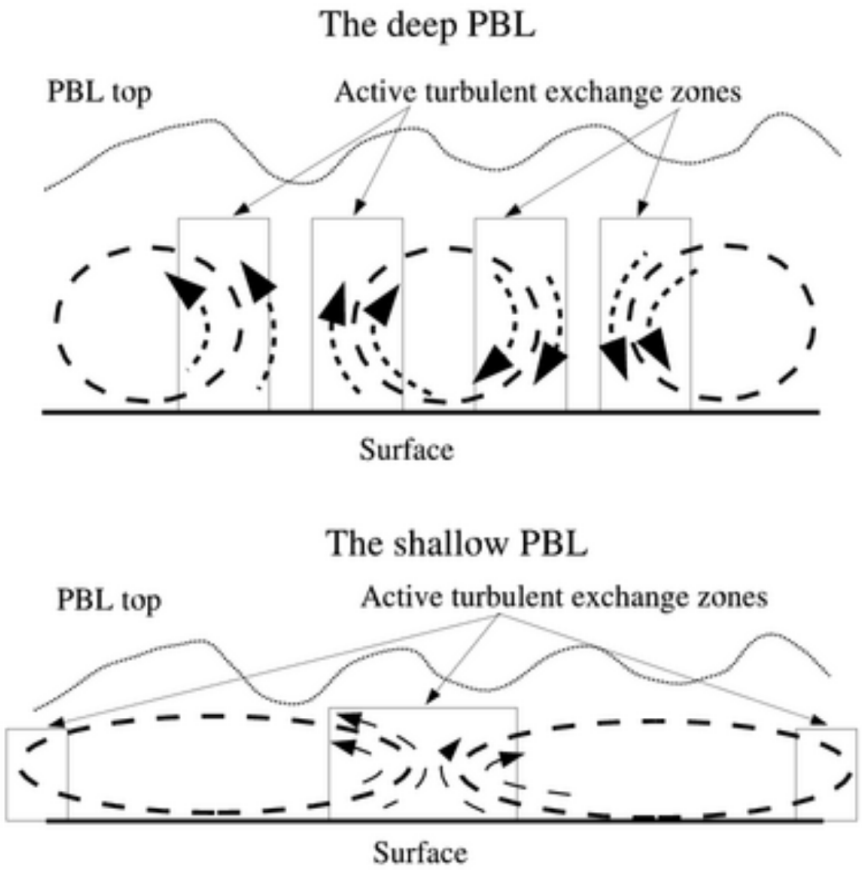

Рис. 6. The sketch of turbulence and turbulent exchange in the surface layer, which are induced by large eddies in the deep PBL (the upper panel) and the shallow PBL (the lower panel).

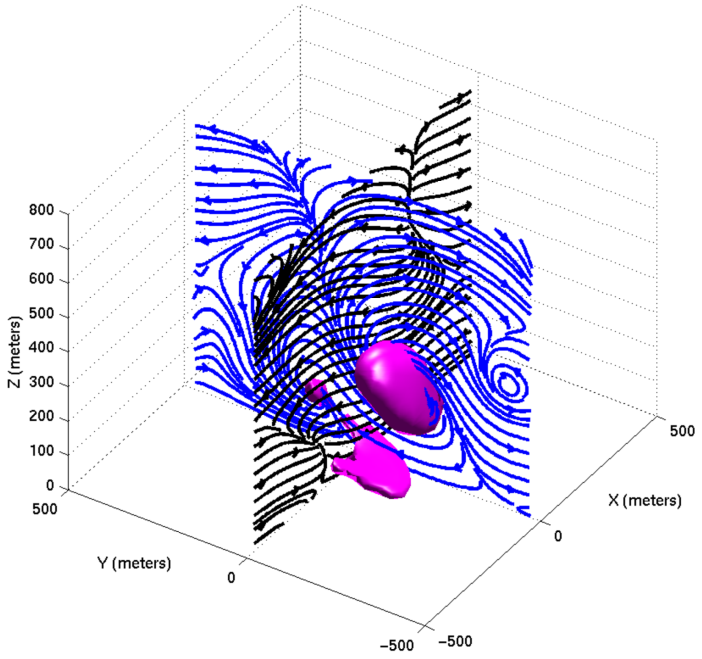

Рис. 7. The typical shape of the statistically most energetic coherent eddy in the truly neutral PBL at the latitude 45° N. Color isosurface shows the absolute value of the horizontal component of the eddy vorticity. Isolines show streamlines of the secondary flow induced by the eddy. The geostrophic wind is directed parallel to the X-axis.

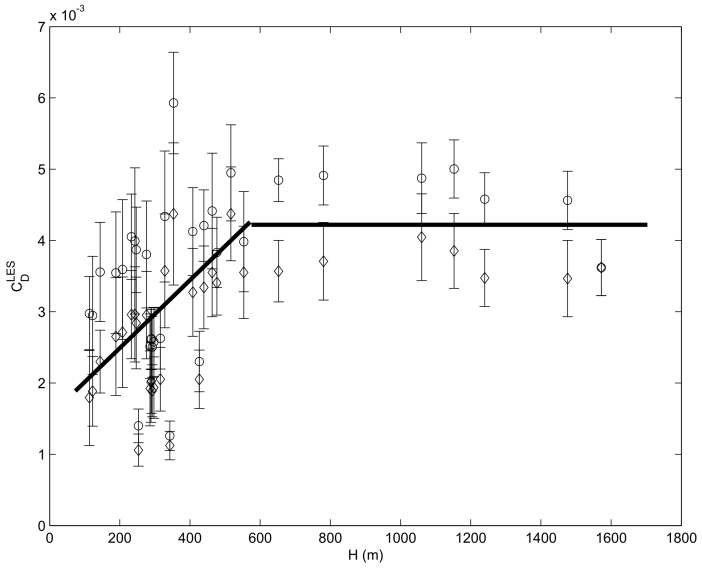

Рис. 8. The dependence of the surface turbulent exchange coefficient C_D^{LES} on the PBL depth H. Symbols and lines are the same as in Fig. 1.

is perhaps some function of f and z_0 as it has been mentioned in the previous Section. Substitution of Eq. (9) into Eq. (7) gives

$$\frac{\partial \mathbf{u}(z)}{\partial z} = \frac{u_*(C_E(z+z_0)+H)}{\kappa(z+z_0)H}. \tag{10}$$

Solving Eq. (10) with the reasonable assumption $z \gg z_0$, one can obtain the following expression for the STEC

$$C_D^H = \frac{\kappa^2}{C_E z/H + \ln(1+\frac{z}{2z_0})} \tag{11}$$

Figure 9 shows C_D^{LES} normalized by the classical local scaling in Eq. (6). Apparently, the local scaling does not work properly in the shallow PBLs. The local scaling results in about twice as much mixing as it is in the LES. Figure 10 shows C_D^{LES} normalized by the non-local scaling in Eq. (11) with $C_E = 7$. Now, C_D^{LES} scales almost perfectly over the whole range of H.

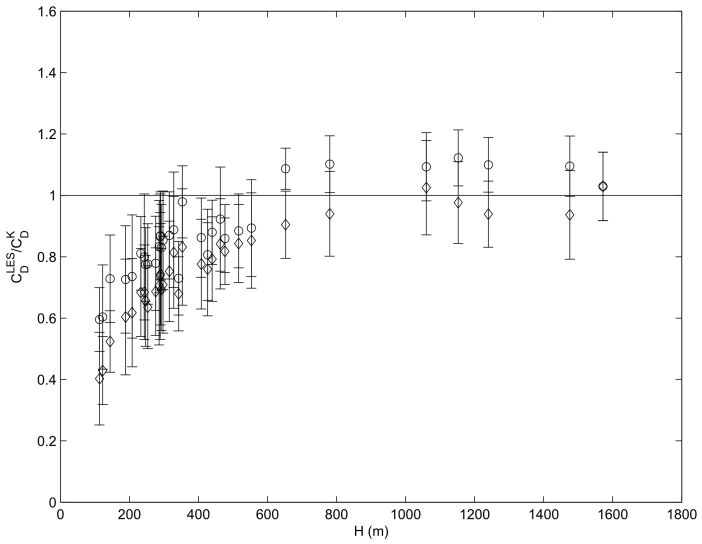

Рис. 9. The ratio C_D^{LES}/C_D^K, where C_D^{LES} is calculated explicitly by Eq. (2) and C_D^K is given by Eq. (3). Symbols and lines are the same as in Fig. (1).

Unfortunately, Eq. (11) cannot be used in the LSMs directly. It contains the unknown parameter H. To express H in terms of resolved variables and boundary conditions, one can involve the Zilitinkevich's generalized equation (8). It gives

$$C_D^H = \frac{\kappa^2}{C_E z(1+C_0\mu_N)^{1/2}|f|/(C_R u_*) + \ln(1+\frac{z}{2z_0})} \tag{12}$$

Now, it is necessary to find an expression for u_*. In Eq. (12), μ_N accounts for the effect of the imposed stability. Thus, it is reasonable to view u_* as the surface turbulent stress, which is induced by the mean wind in a deep PBL. Implicitly, it assumes that the large eddy effect is entirely accounted for through μ_N. This is a strong assumption but it allows the classical log-law in Eq. (3) to employ for the determination of the surface turbulent stress. Substitution

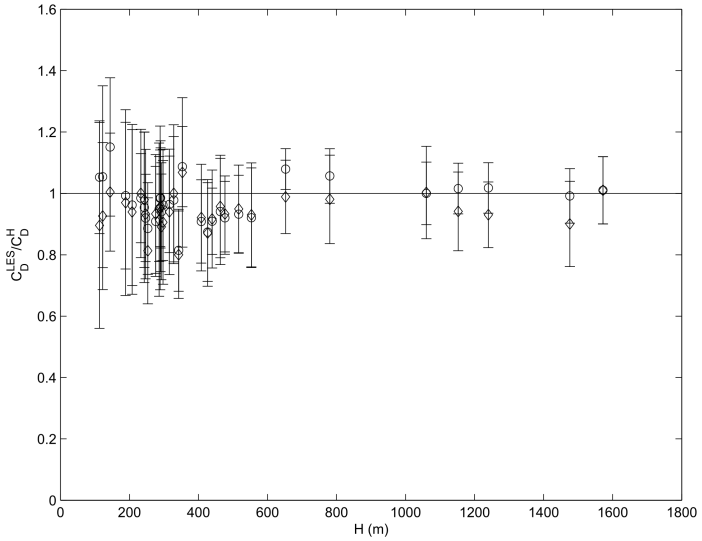

Рис. 10. The ratio C_D^{LES}/C_D^H, where C_D^{LES} is calculated explicitly by Eq. (2) and C_D^H is given by Eq. (11) with $C_E = 7$. Symbols and lines are the same as in Fig. (1).

of Eq. (3) into Eq. (12) provides the final expression for the STEC in terms of the large scale variables

$$C_D^G = \frac{\kappa^2}{C_E^G z(1+C_0\mu_N)^{1/2}|f|\ln(1+\frac{z}{z_0})/(\kappa C_R|\mathbf{u}(z)|), +\ln(1+\frac{z}{2z_0})} \tag{13}$$

where C_E^G is another empirical constant. Figure 11 shows the turbulent exchange coefficient from the LES database normalized by Eq. (13). The comparison of Figures 10 and 11 discloses

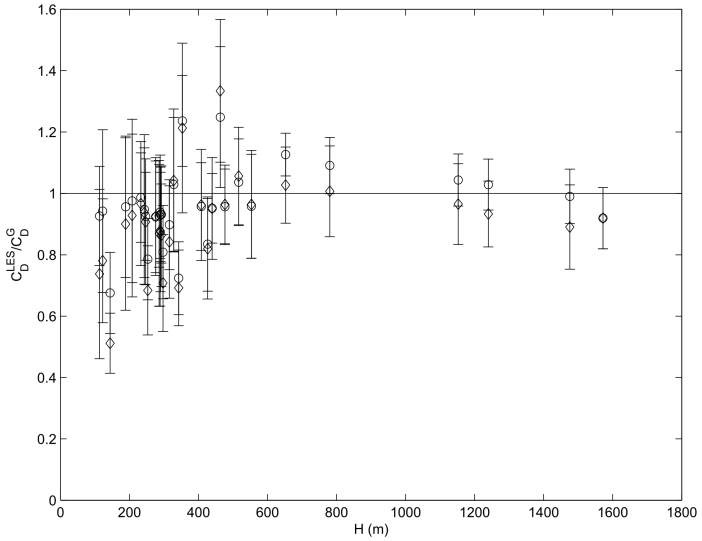

Рис. 11. The ratio C_D^{LES}/C_D^G, where C_D^{LES} is calculated explicitly by Eq. (2) and C_D^G is given by Eq. (13) with $C_E^G = 5$. Symbols and lines are the same as in Fig. (1).

that the above assumptions are not very robust. They result in noticeably larger data scatter. Nevertheless, the scaling by Eq. (13) works better than the classical log-law scaling by Eq. (6). Majority of the LES data scales almost perfectly by Eq. (13) deviating just by $\pm 10\%$ from the analytical curve.

Figure 12 shows the ratio of the classical turbulent exchange coefficient, C_D^K, to the proposed non-local turbulent exchange coefficient, C_D^G. The ratio is close to unity in the deep PBLs (small μ_N) but it rapidly decreases in the shallow PBLs (large μ_N). It is worth to mention that the near-neutral atmospheric PBL has a typically depth less than 400 m [26] and imposed stratification $\mu_N = 100$.

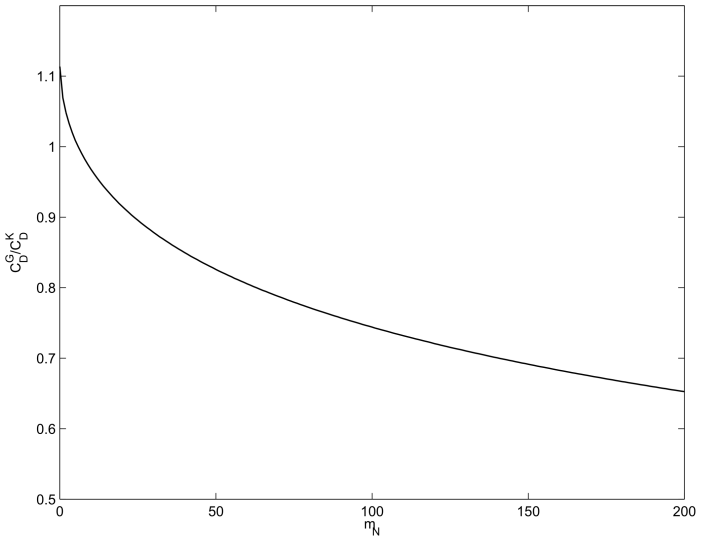

Рис. 12. The ratio of the classical turbulent exchange coefficient, C_D^K, given by Eq. (3), to the proposed non-local turbulent exchange coefficient, C_D^G, given by Eq. (13). Parameters are taken to be $|\mathbf{u}_g| = 5$ m s^{-1}, $z/z_0 = 500$, $C_E^G = 5$, $\kappa = 0.41$ and $\mu_N = 100$.

5. Conclusions

Exploration of the large eddy simulation database reveals that the classical parameterization for the surface turbulent exchange coefficient, C_D, systematically overestimates the turbulent mixing in the conventionally neutral PBLs. The classical parameterization of C_D accounts only for mixing by small scale eddies in the surface layer. The basic assumption is that these small eddies have random spatial distribution and mix the surface layer uniformly.

Additional analysis shows that the large eddies from the PBL core dominate the composition of the surface stress. The large eddies are approximately isotropic in the deep PBL ($H > \Lambda$). The natural scale of the self-organized eddies in the truly neutral PBL is about $\Lambda \approx 600$ m. The shallow PBL ($H < \Lambda$) consists of strongly anisotropic large eddies. Their vertical scale decreases but the horizontal scale changes just slightly. Areas of active turbulent mixing in the surface layer are related to the areas of the strong vertical movements and the areas of the strong horizontal shear. Relative size of these areas decrease with increasing of the eddy anisotropy. This is a possible reason why the shallow PBL has the smaller STEC than it is calculated in the classical log-law theory.

The use of the Blackader's length scale and the Zilitinkevich's PBL-depth equation make possible to include non-local effects into the STEC parameterization. The non-local STEC parameterization demonstrates almost perfect agreement with the LES data over the whole range of the PBL depths. However, the LSMs cannot employ this non-local parameterization since it includes u_* or H as governing parameters.

Some strong additional assumptions about the physical nature of u_* result in suitable computational technology. The suitable computational technology also demonstrates reasonable agreement between the parameterized STEC and the LES data. However, it also demonstrates larger scatter in C_D^G. There is still a hope that the future work will improve this non-local computational technology.

Список литературы

[1] Louis J.F., Tiedtke M. and Geleyn J.F. A short history of the operational PBL parameterization at ECMWF // In *Workshop on planetary boundary layer parameterization*, ECMWF, 25-27 November 1981, 59-80.

[2] Högström U. Review of some characteristics of the atmospheric surface layer // *Boundary Layer Meteorol.*, 1986, **78**, 215-246.

[3] Louis J.F. A parametric model of vertical fluxes in the atmosphere // *Boundary Layer Meteorol.*, 1979, **17**, 187-202.

[4] Zilitinkevich S.S., Perov V.L. and King J.C. Near-surface turbulent fluxes in stable stratification: Calculation for use in general circulation models // *Quart. J. Royal Meteorol. Soc.*, 2002, **128**, 1571-1587.

[5] Monin A.S. and Obukhov A.M. Main characteristics of the turbulent mixing in the atmospheric surface layer // *Trudy Geophys. Inst. AN. SSSR*, 1951, **24**(151), 153-187.

[6] Blackadar A.K. The vertical distribution of wind and turbulent exchange in a neutral atmosphere // *J. Geophys. Res.*, 1962, **67**, 3095-3102.

[7] Rossby C.G. and Montgomery R.B. The Layers of frictional influence in wind and ocean currents // *Pap. Phys. Oceanogr. Meteorol.*, 1935, **3**(3), 101 pp.

[8] Hess G.D. and Garratt J.R. Evaluating models of the neutral, barotropic planetary boundary layer using integral measures: Part I. Overview // *Boundary Layer Meteorol.*, 2002, **104**, 333-358.

[9] Byun D.W. Determination of similarity functions of the resistance laws for the planetary boundary layer using surface layer similarity functions // *Boundary Layer Meteorol.*, 1991, **57**, 17-48.

[10] Zilitinkevich S.S. and Calanca P. An extended similarity-theory for the stably stratified atmospheric surface layer // *Quar. J. Royal Meteorol. Soc.*, 2000, **126**, 1913-1923.

[11] Zilitinkevich S.S. and Esau I.N. On integral measures of the neutral barotropic planetary boundary layer // *Boundary Layer Meteorol.*, 2002, **104**(3), 371-379.

[12] Oncley S.P, Friehe C.A., Larue J.C., Businger J.A., Itsweire E.C. and Chang S.S. Surface-layer fluxes, profiles, and turbulence measurements over uniform terrain under near-neutral conditions // *J. Atmos. Sci.*, 1996, **53**, 1029-1044.

[13] Andreas E.L., Claffey K.J., Fairall C.W., Guest P.S., Jordan R.E. and Persson P.O.G. Evidence from the atmospheric surface layer that the von Karman constant isn't // In *the 15th Symposium on Boundary Layers and Turbulence*, 15-19 July 2002, Wageningen, The Netherlands, 418-421.

[14] Zilitinkevich S.S. Third order transport due to internal waves and non-local turbulence in the stably stratified surface layer // *Quar. J. Royal Meteorol. Soc.*, 2002, **128**(581), 913-925.

[15] Bradshaw P. Inactive motion and pressure fluctuations in turbulent boundary layers // *J. Fluid Mech.*, 1967, **30**, 241-258.

[16] Robinson S.K. Coherent motions in the turbulent boundary layer // *Annu. Rev. Fluid Mech.*, 1991, **23**, 601-639.

[17] Hunt J.C.R. and Morrison J.F. Eddy structure in turbulent boundary layers // *Eur. J. Mech. B-Fluids*, 2000, **19**, 673-694.

[18] Högström U. and Bergström H. Organized turbulence structures in the near-neutral atmospheric surface layer // *J. Atmos. Sci.*, 1996, **53**(17), 2452-2464.

[19] Hunt J.C.R. and Carlotti P. statistical structure at the wall of the high Reynolds number turbulent boundary layer // *Flow, Turbulence and Combustion*, 2001, **66**, 453-475.

[20] Högström U., Hunt J.C.R. and Smedman A.-S. Theory and measurements for turbulence spectra and variances in the atmospheric neutral surface layer // *Boundary Layer Meteorol.*, 2002, **103**, 101-124.

[21] Smagorinsky J. Some historical remarks on the use of nonlinear viscosities // In *Large eddy simulation of complex engineering an geophysical flows*, eds. B. Galperin and S.A. Orszag, 1993, Cambridge Univ. press, pp. 3-34.

[22] Esau I.N. Large eddy simulation database for planetary boundary layer studies. to be submitted in Boundary Layer Meteorol., 2004.

[23] Nastrom G.D. and Gage K.S. Climatology of atmospheric wavenumber spectra of wind and temperature observed by commercial aircraft. *J. Atmos. Sci.*, 1985, **42**(9), 950-960. *J. Atmos. Sci.*, 1990, **47**(16), 1949-1972.

[24] Lin C.-L., Moeng C.-H., Sullivan P.P. and McWilliams J.C. The effect of surface roughness on flow structures in a neutrally stratified planetary boundary layer flow. *Phys. Fluids*, 1997, **9**(11), 3235-3249.

[25] Esau I.N. Coriolis effect on coherent structures in planetary boundary layers. *J. Turbulence*, 2003, **4**, 001.

[26] Stull R.B. *An introduction to boundary layer meteorology*. Kluwer Acad. Press, Dordrecht, The Netherlands, 1988.